Çukurova Üniversitesi
Mühendislik Fakültesi Dergisi
Çukurova University
Journal of the Faculty of Engineering
ISSN: 2757-9255 CİLT/VOLUME: 41 SAYI/ISSUE: 2 HAZİRAN/JUNE 2026

Dynamic Modeling of Scotch Yoke Mechanism with Spring and Mass

Mehmet İlteriş SARIGEÇİLİ [1,a], **İbrahim Deniz AKÇALI** [1,b]

[1]*Çukurova University, Faculty of Engineering, Department of Mechanical Engineering, Adana, Türkiye*

[a]***ORCID**: 0000-0002-9969-2005;* [b]***ORCID**: 0000-0001-5194-5061*

Article Info
Received : 22.12.2025
Accepted : 23.03.2026
DOI: 10.21605/cukurovaumfd.1846971

Corresponding Author
Mehmet İlteriş SARIGEÇİLİ
msarigecili@cu.edu.tr

Keywords
Scotch yoke mechanism
Dynamic model
Sinusoidal compression loading
Parametric assessment

How to cite: *SARIGEÇİLİ, M.İ., AKÇALI, İ.D., (2026). Dynamic Modeling of Scotch Yoke Mechanism with Spring and Mass. Cukurova University, Journal of the Faculty of Engineering, 41(2), 359-370.*

ABSTRACT

Scotch yoke mechanism with a spring and mass can be used to apply a sinusoidal compression force on a specimen by converting rotational motion from an electric motor into reciprocating motion. The dynamic model of such a mechanism considering friction and variable speed effects has been developed in this study. A Python code has been written for the dynamic model to solve for the required input torque and joint forces based on the input motion characteristics. By changing the values of some parameters of the dynamic model, 7 different groups are defined to observe the effects of these parameters on the required input torque, joint force and spring compression force values. The associated graphs drawn in the time domain have been analyzed to cast light on the rational choice of these parameters.

Bir Yay ve Kütle İçeren Scotch Yoke Mekanizmasının Dinamik Modellemesi

Makale Bilgileri
Geliş : 22.12.2025
Kabul : 23.03.2026
DOI: 10.21605/cukurovaumfd.1846971

Sorumlu Yazar
Mehmet İlteriş SARIGEÇİLİ
msarigecili@cu.edu.tr

Anahtar Kelimeler
Scotch yoke mekanizması
Dinamik model
Sinüzoidal basma yüklemesi
Parametrik değerlendirme

Atıf şekli: *SARIGEÇİLİ, M.İ., AKÇALI, İ.D., (2026). Bir Yay ve Kütle İçeren Scotch Yoke Mekanizmasının Dinamik Modellemesi. Çukurova Üniversitesi, Mühendislik Fakültesi Dergisi, 41(2), 359-370.*

ÖZ

Bir yay ve kütle içeren Scotch yoke mekanizması, elektrik motorundan sağlanan dönme hareketini gidip gelme hareketine çevirerek, sinüzoidal bir basma yüklemesi elde etmek için kullanılabilir. Bu çalışmada, böyle bir mekanizmanın sürtünme ve hızdaki değişme etkileri de düşünülerek dinamik modeli geliştirilmiştir. Giriş hareket karakteristiklerine bağlı olarak ihtiyaç duyulan giriş torkunun ve mafsal kuvvetlerinin hesaplanması için Python dilinde bir program hazırlanmıştır. Dinamik modeldeki parametrelerin ihtiyaç duyulan giriş torku, mafsal ve yay basma kuvvetleri üzerindeki etkilerinin gözlemlenmesi için ilgili parametre değerlerinin değiştirildiği 7 farklı grup oluşturulmuştur. Zaman bölgesinde çizilen grafikler üzerinden ilgili parametre değerlerinin uygun seçilmesine ışık tutacak şekilde değerlendirmeler yapılmıştır.

1. INTRODUCTION

Scotch yoke and slider-crank mechanisms both convert rotational motion into translational motion or vice versa even though Scotch yoke is preferred for smoother motion characteristics. Hence, there are many design applications utilizing Scotch yoke mechanism. For example, Scotch yoke with a spring mechanism [1] has been utilized in the design of a one degree-of-freedom rotary system gravity balancer. Al Shami et al. [2] and Hossain et al. [3] developed a wave energy harvester from a Scotch yoke mechanism. Subramanian et al. [4] made use of a Scotch yoke mechanism to develop a two-way pumping system while Rivankar et al. [5] proposed a modified Scotch yoke based polishing machine.

Scotch yoke mechanisms have non-linear dynamics. The modeling approaches are well studied for producing constant torque output, controlling the output speed as well as converting the linear excitation motion into torque output. For example, a Scotch yoke mechanism was used to give tail fin motion of a robotic fish design by Kwon [6]. The motor output torque was controlled by utilizing an adjustable Scotch yoke mechanism with crank wheel which was designed as a cam with springs. Prastiyo and Fiebig [7] developed the dynamic model of both slider-crank and Scotch yoke mechanisms by means of Euler-Lagrange method. They came to the conclusion that inertia forces, moments and torques are reduced drastically when these mechanisms are operated under angular speeds corresponding to resonance conditions. Rayed et al. [8] utilized a Scotch yoke based mechanism for mimicking the flapping of a bird. In that study, FEM analysis of stress, deformation and fatigue life were performed to figure out the critical sections and furthermore topology optimization was applied to the base. Liang and Liu [9] carried out dynamic analysis of Scotch yoke mechanism with configurations of a single piston, opposed double piston and inclined slot by simulating in ADAMS. Tao et al. [10] designed a Limacon gear driven Scotch yoke mechanism in order to obtain uniform reciprocating motion of a forming device of the carding machine. In addition, modified genetic algorithm was applied with the objective of lowering the average velocity of the guide (i.e. yoke). Apati and Hegedus [11] developed electromechanical model of a battery-powered jigsaw using a Scotch yoke mechanism, where Lagrange equation is utilized to analyze the force-energy relationship based on the considerations of both kinetic and magnetic co-energy. The motor speed, current consumption and blade movement under different cutting loads are obtained with the developed simulation program. Al-Hamood et al. [12] used dynamic model of a Scotch yoke mechanism to investigate the contact problem under elastohydrodynamic lubrication by means of a line contact model based on non-Newtonian oil behavior, varying loads, and surface velocities throughout the operating cycle. Tai et al. [13] designed a Scotch yoke based nonlinear vibration isolator. The dynamic model of the system was developed for the motion equation of the coupled structure-vibration isolator. The simulation results of the dynamic analysis for various parameters such as amplitude-frequency response, the critical excitation amplitude, etc. were presented. In addition to dynamic model studies of Scotch yoke mechanisms, models of slider-crank mechanisms are also well studied. As an example, the kinematic analysis of a slider-crank mechanism in a tractor motor has been done in MSC ADAMS software by Beyaz and Dağtekin [14]. In another study, dynamic model of a slider-crank mechanism has been developed with lumped mass approach for the analysis of the piston speed by Sarıgeçili and Akçalı [15]. That mechanism has specifically a helical spring attached to the crank center and a force applied onto the crank-pin.

An outstanding feature of the Scotch yoke mechanism is that motion conversion from a constantly rotating crank to the translating slider takes place in a perfectly sinusoidal form. This feature of the mechanism is utilized in [16] to develop a conceptual design model of an axial fatigue loading machine. However, in that study not only the friction, which is inevitably present in the system and critically affects the operation of this mechanism, was not considered but also the angular velocity of the crank was assumed to be constant. The main objective of this study is to develop a dynamic model of a Scotch yoke mechanism with a spring and mass by taking into account both the friction and variable crank speed effects. In this way, the foundation by which the response of the system model to different sets of parameter values in terms of input torque, compressive spring force on a specimen and significant joint forces is estimated, will be laid down for a rational selection of these parameters according to the prescribed criteria.

2. DYNAMIC MODEL

Schematic representation of Scotch yoke mechanism with spring and mass, in which a compression force is applied against a specimen, is shown in Figure 1. The ground, crank, slider and yoke are represented by 1, 2, 3 and 4, respectively. Since the frictional force direction is always opposite to the motion direction and both of the sliding motions (i.e. slider and yoke) change direction in a full cycle, dynamic analysis of a Scotch yoke mechanism has to be performed separately for each quadrant of the crank angle as shown in Figure 1.a through 1.d together with free body diagrams of each component. In addition, for accuracy in the model, these analyses are to be revised at every critical point of 0°, 90°, 180°, 270°, 360° crank angle, where the relative velocity between either the intermediate slider (3) and the yoke (4) or that between the yoke (4) and the ground (1) becomes instantly zero. In the schematic representation of the Scotch yoke mechanism, the crank length from point O to point A is represented by r and the crank angle is shown by θ. The distance from vertical sliding joints of points M and N to crank center O is presented by l_M and l_N, respectively. The thickness of the slider slot along y-axis is t_1 and yoke thickness is t_2. The friction coefficients between the slider & the slot, and the yoke & the ground are μ_1 and μ_2, respectively. The spring at the bottom of the yoke has a spring constant of k and an initial compression of x_0. Any attached weight including the yoke weight is represented by W. The crank is assumed to have a mass center at O with mass moment of inertia I_2.

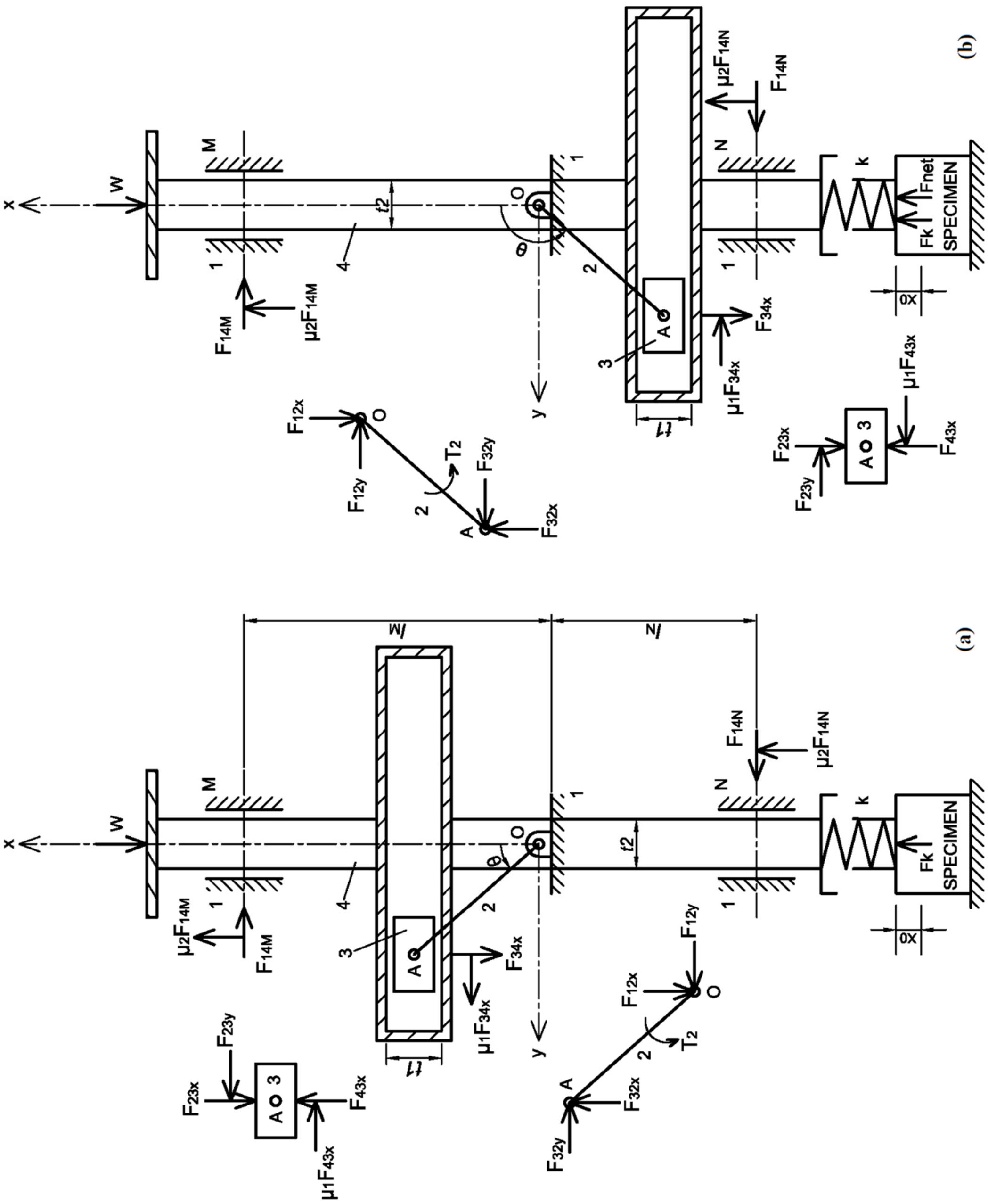

Figure 1. Schematic representation of Scotch yoke mechanism

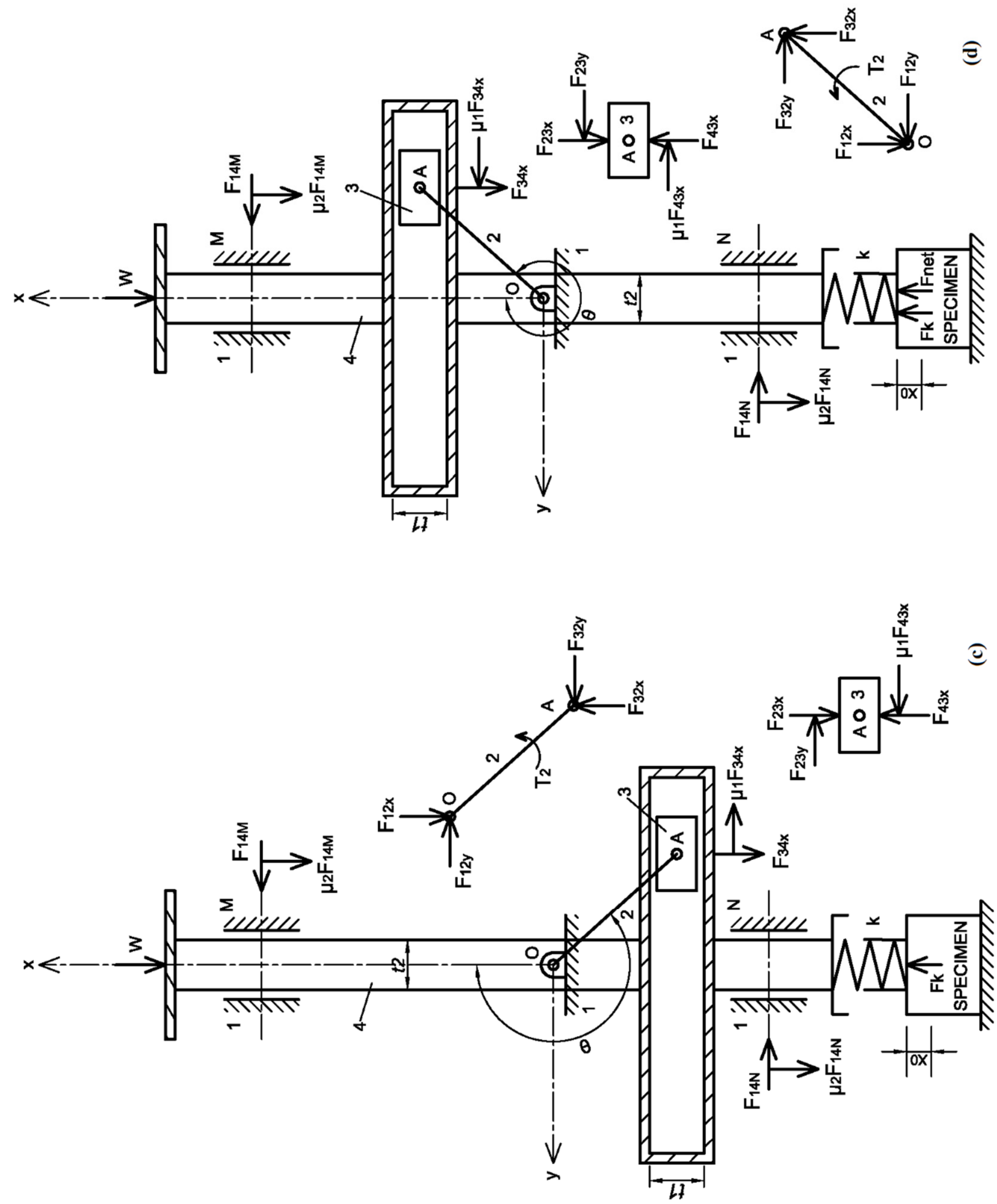

Figure 1. (continue)

The frictional effects due to relative rotation at the revolute joints of the crank are assumed to be negligible. On the other hand, frictional forces due to relative sliding between slider and yoke as well as between yoke and ground are taken into account based on Coulomb friction model. It should be reminded that the coefficient of static friction is in effect at the start of motion and the coefficient of kinetic friction (which is lower than the coefficient of static friction) is in effect while in motion. Also, frictional forces are not constant and they change throughout the mating surfaces. However, in this study, an average coefficient of static friction is used in the dynamic model to be able to choose the right electric motor the power of which is enough to overcome the frictional effects in running the mechanism.

The position (x) and displacement (Δx) of the output link in the Scotch yoke mechanism along vertical x axis are described by Equations (1) and (2), respectively. The speed ($\dot{x}$) in Equation (3) and acceleration ($\ddot{x}$) in Equation (4) are found by taking the first and second time derivative of the position equation, respectively.

$$x = r\cos\theta \tag{1}$$

$$\Delta x = r - r\cos\theta = r(1-\cos\theta) \tag{2}$$

$$\dot{x} = -r\dot{\theta}\sin\theta \tag{3}$$

$$\ddot{x} = -r\dot{\theta}^2\cos\theta - r\ddot{\theta}\sin\theta \tag{4}$$

The crank in the Scotch yoke mechanism is required to run at a constant input angular speed (ω) to produce a perfect sinusoidal rectilinear reciprocating motion as the output. However, the system starts from rest and there should be an angular acceleration (α) until the constant angular speed is reached. Hence, the input motion, as shown in Figure 2, is modeled as starting motion from rest at a constant angular acceleration at t_0 until the specified constant speed ω is obtained at t_1. Thereafter, the input motion is supposed to continue with zero angular acceleration.

The force analysis procedures followed in this study with the motion characteristics presented in Figure 2 are given below:

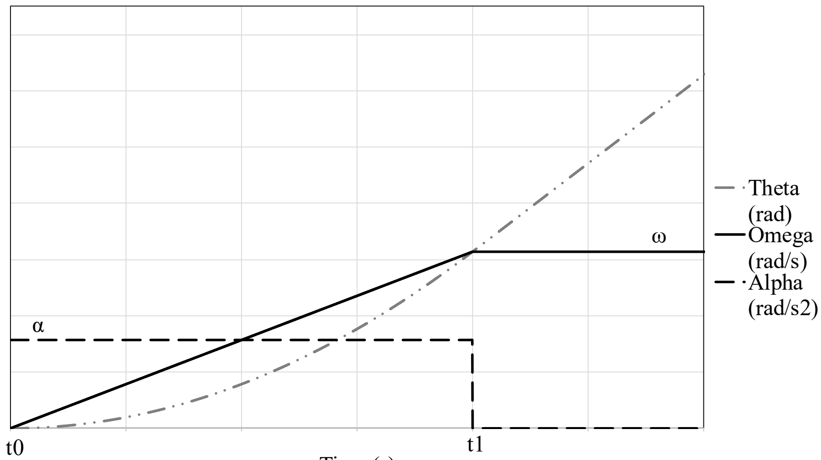

Figure 2. Input motion characteristics: Angular acceleration (α), speed (ω) and position (θ) of the crank in time domain

1. The analysis is started from link 3. Total forces along x and y should be zero.

$$F_{ij}^{x} = -F_{ji}^{x},\ ij = 32, 21, 43 \tag{5}$$

$$F_{ij}^{y} = \mu_1 F_{ij}^{x},\ ij = 32, 21, 43 \tag{6}$$

$$F_{ij}^{y} = -F_{ji}^{y},\ ij = 32, 21, 43 \tag{7}$$

2. The analysis is followed by link 2. Total forces along x and y as well as total moment about point O are zero. The relation between the joint force exerted by link 3 onto link 2 (F_{32}^{x}) and torque applied to link 2 (T_2) are found out.

3. Then, the analysis on link 4 is carried out. Total forces along x and y axes as well as total moment about point O are zero. Ground reaction forces F_{14M} and F_{14N} along y axis are determined. These expressions are substituted into the governing (Newton) equation from which torque T_2 is solved.

4. Once T_2 is determined, final formulae for F_{34}^{x}, F_{14M} and F_{14N} easily follow. F_{14M}^{x} and F_{14N}^{x} are expressed as such:

$$F_{14i}^{x} = \mu_2 F_{14i}\ ,\ i = M, N \tag{8}$$

5. The yoke has no instant motion for $\theta = 0$ and $\theta = \pi$. Therefore, the frictional forces along joints M and N have to be zero.

$$F_{14i}^{x} = 0\,,\ i = M, N \tag{9}$$

6. Also, the slider has no instant relative motion for $\theta = \pi/2$ and $\theta = 3\pi/2$. Hence, the slider friction force has to be zero.

$$F_{ij}^{y} = F_{ji}^{y} = 0,\ \ ij = 32, 21, 43 \tag{10}$$

Application of these procedures yield the following relationships for T_2, F_{32}^{x}, F_{14M} and F_{14N} in terms of the crank angular positions indicated below and the other unknown quantities can be found by Equations (5)-(8):

- $\boldsymbol{\theta = 0 + 2\pi n, n = 0, 1, 2, \ldots}$

$$T_2 = \left(-W + \frac{W}{g} r\dot{\theta}^2 + kx_0\right)\mu_1 r + I_2\alpha \tag{11}$$

$$F_{32}^{x} = \frac{T_2 - I_2\alpha}{\mu_1 r} \tag{12}$$

$$F_{14M} = \frac{T_2 - I_2\alpha}{r(l_M + l_N)}\left(r - \frac{t_1}{2} + l_N\right) \tag{13}$$

$$F_{14N} = \frac{T_2 - I_2\alpha}{r(l_M + l_N)}\left(r - \frac{t_1}{2} - l_M\right) \tag{14}$$

$$F_{14M}{}^{x} = F_{14N}{}^{x} = 0 \tag{15}$$

- $\boldsymbol{0 < \theta < (\pi/2 + 2\pi n), n = 0, 1, 2, \ldots}$

Call A_1 as:

$$A_1 = \frac{1}{r\sin\theta + \mu_1 r\cos\theta}\left[1 - \frac{\mu_2(2r\sin\theta + 2\mu_1 r\cos\theta - \mu_1 t_1 - \mu_1\mu_2 t_2 + \mu_1 l_N - \mu_1 l_M)}{(l_M + l_N)}\right] \tag{16}$$

$$T_2 = \left(-W - \frac{W}{g}\left(-r\dot{\theta}^2\cos\theta - r\ddot{\theta}\sin\theta\right) + kx_0 + kr(1 - \cos\theta)\right)\frac{1}{A_1} + I_2\ddot{\theta} \tag{17}$$

$$F_{32}^{x} = \frac{T_2 - I_2\alpha}{r\sin\theta + \mu_1 r\cos\theta} \tag{18}$$

$$F_{14M} = \frac{(T_2 - I_2\alpha)\left(r\sin\theta + \mu_1 r\cos\theta - \mu_1\frac{t_1}{2} - \mu_1\mu_2\frac{t_2}{2} + \mu_1 l_N\right)}{(l_M + l_N)(r\sin\theta + \mu_1 r\cos\theta)} \tag{19}$$

$$F_{14N} = \frac{(T_2 - I_2\alpha)\left(r\sin\theta + \mu_1 r\cos\theta - \mu_1\frac{t_1}{2} - \mu_1\mu_2\frac{t_2}{2} - \mu_1 l_M\right)}{(l_M + l_N)(r\sin\theta + \mu_1 r\cos\theta)} \tag{20}$$

- $\boldsymbol{\theta = \pi/2 + 2\pi n, n = 0, 1, 2, \ldots}$

$$T_2 = \left(-W + \frac{W}{g}\left(r\ddot{\theta}\right) + kx_0 + kr\right)\frac{(l_M + l_N)r}{l_M + l_N - 2\mu_2 r} + I_2\alpha \tag{21}$$

$$F_{32}^{x} = \frac{T_2 - I_2\alpha}{r} \tag{22}$$

$$F_{32}^{y} = 0 \tag{23}$$

$$F_{14M} = F_{14N} = \frac{T_2 - I_2\alpha}{(l_M + l_N)} \tag{24}$$

- $\boldsymbol{(\pi/2 + 2\pi n) < \theta < (\pi + 2\pi n), n = 0, 1, 2, \ldots}$

Call A_2 as:

$$A_2 = \frac{1}{r\sin\theta - \mu_1 r\cos\theta}\left[1 - \frac{\mu_2(2r\sin\theta - 2\mu_1 r\cos\theta + \mu_1 t_1 + \mu_1\mu_2 t_2 - \mu_1 l_N + \mu_1 l_M)}{(l_M + l_N)}\right] \quad (25)$$

$$T_2 = \frac{\left[-W - \frac{W}{g}(-r\dot{\theta}^2\cos\theta - r\ddot{\theta}\sin\theta) + kx_0 + kr(1-\cos\theta)\right]}{A_2} + I_2\alpha \quad (26)$$

$$F_{32}^x = \frac{T_2 - I_2\alpha}{r\sin\theta - \mu_1 r\cos\theta} \quad (27)$$

$$F_{14M} = \frac{(T_2 - I_2\alpha)\left(r\sin\theta - \mu_1 r\cos\theta + \mu_1\frac{t_1}{2} + \mu_1\mu_2\frac{t_2}{2} - \mu_1 l_N\right)}{(r\sin\theta - \mu_1 r\cos\theta)(l_M + l_N)} \quad (28)$$

$$F_{14N} = \frac{(T_2 - I_2\alpha)\left(r\sin\theta - \mu_1 r\cos\theta + \mu_1\frac{t_1}{2} + \mu_1\mu_2\frac{t_2}{2} + \mu_1 l_M\right)}{(r\sin\theta - \mu_1 r\cos\theta)(l_M + l_N)} \quad (29)$$

- $\boldsymbol{\theta = \pi + 2\pi n, n = 0, 1, 2, \ldots}$

$$T_2 = \left(-W - \frac{W}{g}r\dot{\theta}^2 + kx_0 + 2kr\right)\mu_1 r + I_2\alpha \quad (30)$$

$$F_{32}^x = \frac{T_2 - I_2\alpha}{\mu_1 r} \quad (31)$$

$$F_{14M} = \frac{\mu_1 F_{34}^x}{(l_M + l_N)}\left(r + \frac{t_1}{2} - l_N\right) \quad (32)$$

$$F_{14N} = \frac{\mu_1 F_{34}^x}{(l_M + l_N)}\left(r + \frac{t_1}{2} + l_M\right) \quad (33)$$

$$F_{14M}{}^x = F_{14N}{}^x = 0 \quad (34)$$

- $\boldsymbol{(\pi + 2\pi n) < \theta < (3\pi/2 + 2\pi n), n = 0, 1, 2, \ldots}$

Call A_3 as:

$$A_3 = \frac{1}{r\sin\theta - \mu_1 r\cos\theta}\left[1 - \frac{\mu_2(2r\sin\theta - 2\mu_1 r\cos\theta + \mu_1 t_1 - \mu_1\mu_2 t_2 + \mu_1 l_M - \mu_1 l_N)}{(l_M + l_N)}\right] \quad (35)$$

$$T_2 = \frac{\left[-W - \frac{W}{g}(-r\dot{\theta}^2\cos\theta - r\ddot{\theta}\sin\theta) + kx_0 + kr(1-\cos\theta)\right]}{A_3} + I_2\alpha \quad (36)$$

$$F_{32}^x = \frac{T_2 - I_2\alpha}{r\sin\theta - \mu_1 r\cos\theta} \quad (37)$$

$$F_{14M} = -\frac{(T_2 - I_2\alpha)\left(r\sin\theta - \mu_1 r\cos\theta + \mu_1\frac{t_1}{2} - \mu_1 l_N - \mu_1\mu_2\frac{t_2}{2}\right)}{(r\sin\theta - \mu_1 r\cos\theta)(l_M + l_N)} \quad (38)$$

$$F_{14N} = -\frac{(T_2 - I_2\alpha)\left(r\sin\theta - \mu_1 r\cos\theta + \mu_1\frac{t_1}{2} - \mu_1\mu_2\frac{t_2}{2} + \mu_1 l_M\right)}{(r\sin\theta - \mu_1 r\cos\theta)(l_M + l_N)} \quad (39)$$

- $\boldsymbol{\theta = 3\pi/2 + 2\pi n, n = 0, 1, 2, \ldots}$

Call A_4 as:

$$A_4 = \frac{1}{r}\left(1 + \frac{2\mu_2 r}{(l_M + l_N)}\right) \quad (40)$$

$$T_2 = \frac{\left(W+\frac{W}{g}(r\ddot{\theta})-kx_0-kr\right)}{A_4} + I_2\alpha \tag{41}$$

$$F_{32}^x = -\frac{T_2-I_2\alpha}{r} \tag{42}$$

$$F_{32}^y = 0 \tag{43}$$

$$F_{14M} = F_{14N} = -\frac{T_2-I_2\alpha}{(l_M+l_N)} \tag{44}$$

- $\boldsymbol{(3\pi/2+2\pi n) < \theta < (2\pi+2\pi n), n = 0, 1, 2, \ldots}$

Call A_5 as:

$$A_5 = \frac{1}{r\sin\theta+\mu_1 r\cos\theta}\left[1-\frac{\mu_2(2r\sin\theta+2\mu_1 r\cos\theta-\mu_1 t_1+\mu_1\mu_2 t_2+\mu_1 l_N-\mu_1 l_M)}{(l_M+l_N)}\right] \tag{45}$$

$$T_2 = \frac{\left(-W-\frac{W}{g}(-r\dot{\theta}^2\cos\theta-r\ddot{\theta}\sin\theta)+kx_0+kr(1-\cos\theta)\right)}{A_5} + I_2\alpha \tag{46}$$

$$F_{32}^x = \frac{T_2-I_2\alpha}{r\sin\theta+\mu_1 r\cos\theta} \tag{47}$$

$$F_{14M} = -\frac{(T_2-I_2\alpha)\left(r\sin\theta+\mu_1 r\cos\theta-\mu_1\frac{t_1}{2}+\mu_1 l_N+\mu_1\mu_2\frac{t_2}{2}\right)}{(r\sin\theta+\mu_1 r\cos\theta)(l_M+l_N)} \tag{48}$$

$$F_{14N} = -\frac{(T_2-I_2\alpha)\left(r\sin\theta+\mu_1 r\cos\theta-\mu_1\frac{t_1}{2}+\mu_1\mu_2\frac{t_2}{2}-\mu_1 l_M\right)}{(r\sin\theta+\mu_1 r\cos\theta)(l_M+l_N)} \tag{49}$$

3. RESULTS AND DISCUSSION

A Python code has been written to obtain the numerical results from the developed dynamic system model. In calculations, the crank is accepted to start rotational motion from θ = 0° position at rest with constant angular acceleration until the final angular speed (ω_f) is reached and thereafter is to continue with zero angular acceleration. The analysis of the model has been carried out within a selected duration of 5 s with computations being repeated for every 0.01 s time increments. For this purpose, 7 different groups of parameters have been defined as given in Table 1. These groups of parameters have been selected specifically for fatigue loading machine such that the compression force exerted by the slider on the yoke (F_{34}^x) does not have negative values. Otherwise the model becomes invalid with a joint force pulling up instead of pushing down. Also, the other parameters are arranged such that the crank can be rotated fully.

Table 1. Parameters for the analysis of the model

Group name	Parameters
G1	x_0 = 0.018 m, W = 40 N, r = 0.022 m, k = 2500 N/m, I_2 = 5 kg·m^2, α = 3.14 rad/s^2, ω_0 = 0 rad/s, ω_f = 6.28 rad/s, t_f = 5s, Δt = 0.01 s, μ_1 = 0.1, μ_2 = 0.1
G2	x_0 = 0.018 m, W = 30 N, r = 0.022 m, k = 2500 N/m, I_2 = 5 kg·m^2, α = 3.14 rad/s^2, ω_0 = 0 rad/s, ω_f = 6.28 rad/s, t_f = 5s, Δt = 0.01 s, μ_1 = 0.1, μ_2 = 0.1
G3	x_0 = 0.018 m, W = 40 N, r = 0.030 m, k = 2500 N/m, I_2 = 5 kg·m^2, α = 3.14 rad/s^2, ω_0 = 0 rad/s, ω_f = 6.28 rad/s, t_f = 5s, Δt = 0.01 s, μ_1 = 0.1, μ_2 = 0.1
G4	x_0 = 0.018 m, W = 40 N, r = 0.022 m, k = 2500 N/m, I_2 = 2.5 kg·m^2, α = 3.14 rad/s^2, ω_0 = 0 rad/s, ω_f = 6.28 rad/s, t_f = 5s, Δt = 0.01 s, μ_1 = 0.1, μ_2 = 0.1
G5	x_0 = 0.018 m, W = 40 N, r = 0.022 m, k = 5000 N/m, I_2 = 5 kg·m^2, α = 3.14 rad/s^2, ω_0 = 0 rad/s, ω_f = 6.28 rad/s, t_f = 5s, Δt = 0.01 s, μ_1 = 0.1, μ_2 = 0.1
G6	x_0 = 0.025 m, W = 40 N, r = 0.022 m, k = 2500 N/m, I_2 = 5 kg·m^2, α = 3.14 rad/s^2, ω_0 = 0 rad/s, ω_f = 6.28 rad/s, t_f = 5s, Δt = 0.01 s, μ_1 = 0.1, μ_2 = 0.1
G7	x_0 = 0.018 m, W = 40 N, r = 0.022 m, k = 2500 N/m, I_2 = 5 kg·m^2, α = 3.14 rad/s^2, ω_0 = 0 rad/s, ω_f = 12.56 rad/s, t_f = 5s, Δt = 0.01 s, μ_1 = 0.1, μ_2 = 0.1

By running the Python code for each group of parameters, the required input torque, joint forces and the spring compression force on the specimen are evaluated. Due to space limitations, only input torque (T_2), joint force (F_{34}^x) and spring force (F_k) graphs drawn in the selected time domain have been presented for the review of the numerical results.

The required torque T_2 vs. time graphs are shown in Figure 3. It can be seen from the graphs that increasing crank radius r (G3 graph) and spring constant k (G5 graph) leads to an increase in the torque value. A reduction in the mass moment of inertia I_2 (G4 graph) reduces the required torque value in the constant acceleration region, whereas in the constant speed region the required torque value remains unchanged. Increasing the constant speed value (G7 graph) just extends the high torque value region to the point where the constant speed region begins. It appears that the other parameters do not have significant effect on the required torque.

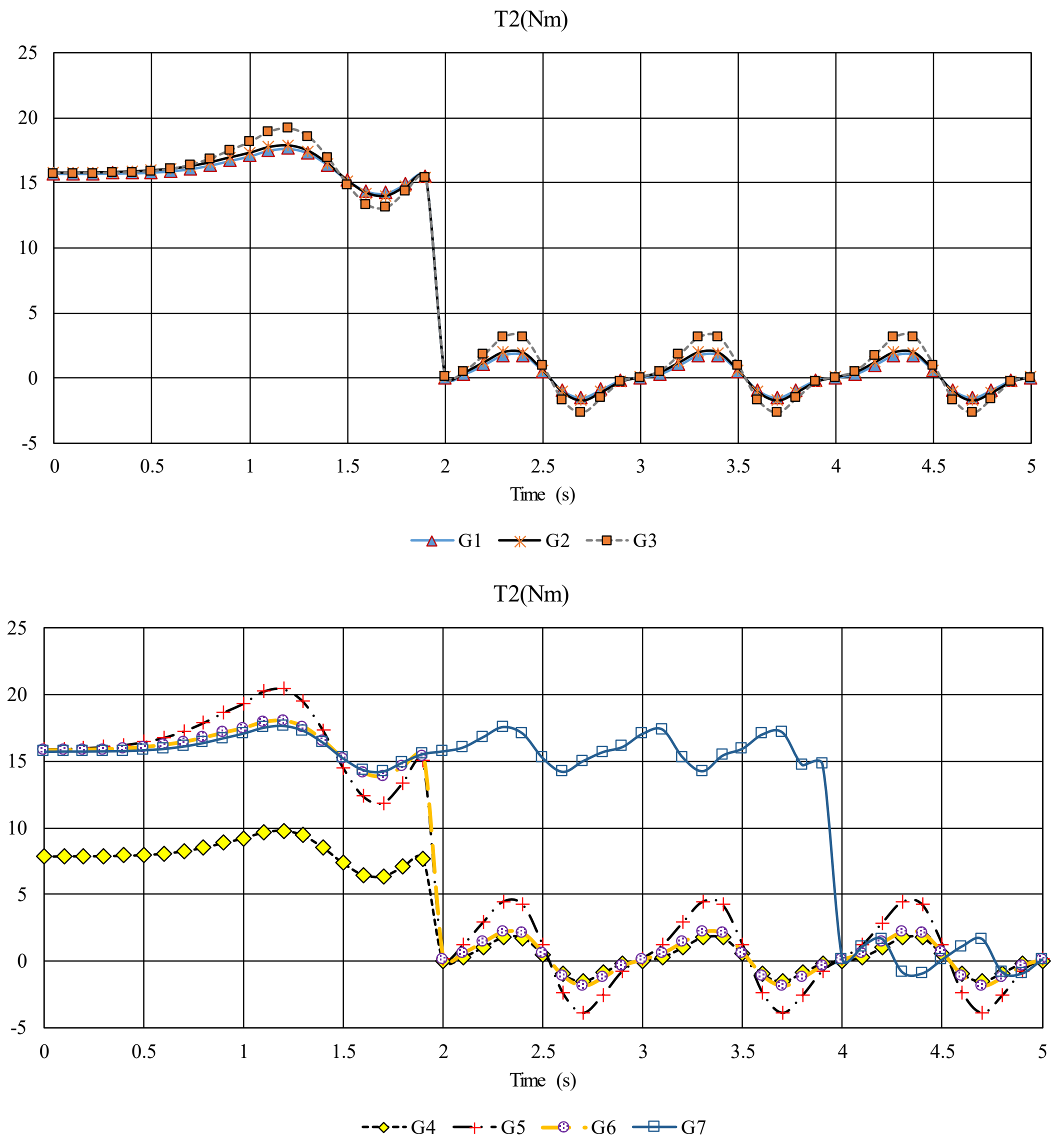

Figure 3. Input torque (T_2) vs time graph

The joint force F_{34}^x vs. time graphs are shown in Figure 4. A reduction in weight W (G2 graph), an increase in crank radius r (G3 graph), an increase in spring constant k (G5 graph) and an increase in initial spring compression x_0 (G6 graph) increase F_{34}^x. A change in the mass moment of inertia I_2 (G4 graph) and the constant speed value (G7 graph) do not seem to change maximum and minimum values of F_{34}^x. However, the angular speed changes the frequency of F_{34}^x.

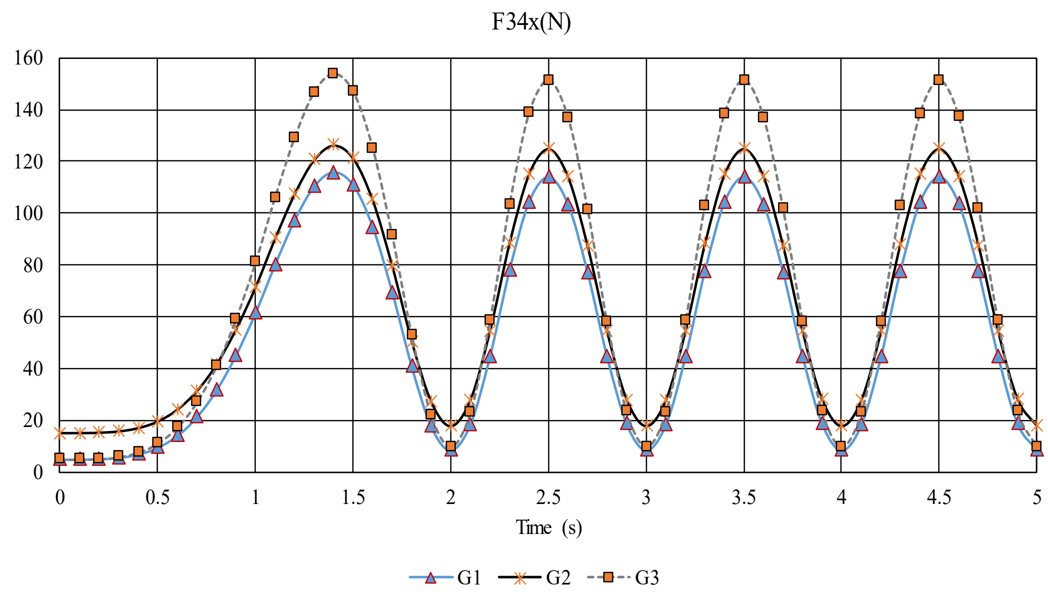

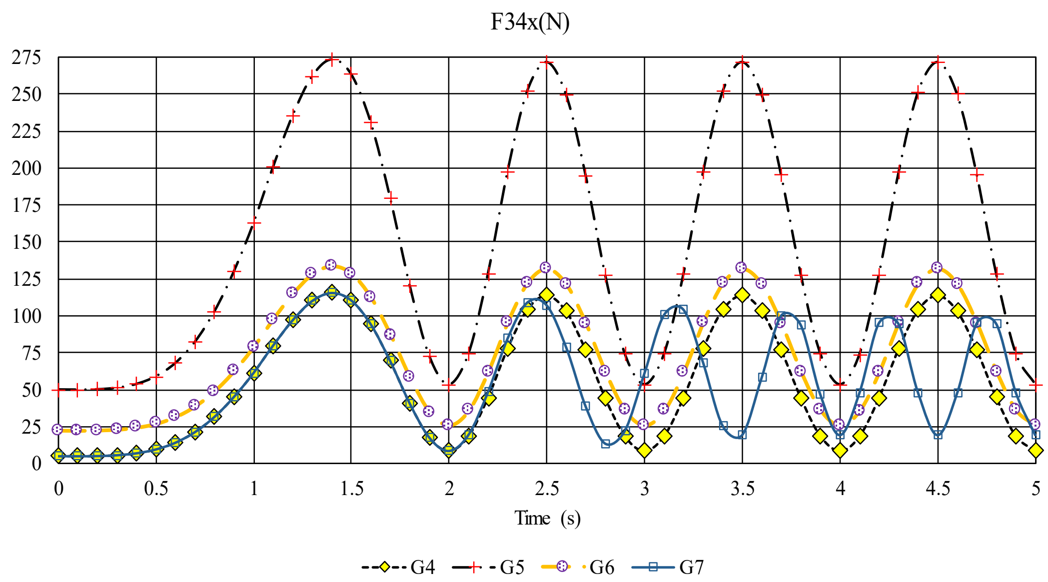

Figure 4. Joint force (F_{34x}) vs time graph

In Figure 5, the spring compression force F_k vs. time graphs are presented. From the graphs, it is clear that increasing crank radius r (G3 graph), spring constant k (G5 graph) and initial spring compression x_0 (G6 graph) results in an increase in F_k. Nevertheless, an increase in x_0 only shifts the maximum and minimum values of the spring force upwards by the same amount during which the amplitude of variation remains unaffected, while changes in the spring constant and crank radius influence both the maximum value and amplitude of spring force. The other parameters do not seem to affect F_k except that the angular speed causes a change in the frequency.

A designer can change as necessary as required the parameters in the dynamic model and run the code to see the effects on the results of particular requirements. The designer would realize that;

- increasing the spring constant k, crank radius r and initial spring compression x_0 raises the joint force F_{34}^{x} to an irrational value which hinders the 360-degree rotation of the crank,
- bearing loads can be analyzed and the parameters can be selected for smaller bearing reactions,
- input torque values can be analyzed for the selection of a suitable electric motor.

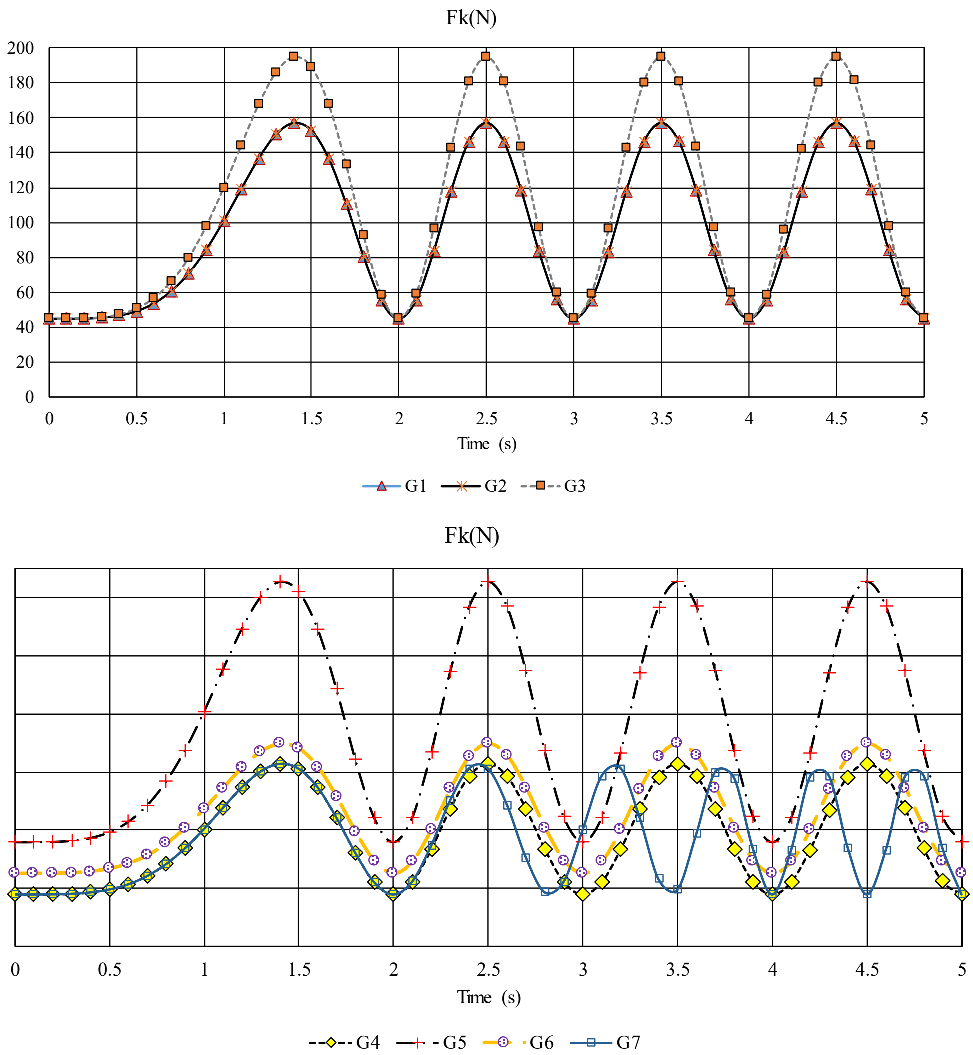

Figure 5. Spring force (F_k) vs time graph

4. CONCLUSION

In this study, the dynamic model of a Scotch yoke mechanism with spring and mass has been developed. The friction effects on the intermediate slider-yoke and on the yoke-ground interfaces as well as variable crank speed effects have also been considered. The developed model predicts the values of the required input torque, joint forces and spring compression force when the input motion characteristics and values of the system parameters are specified. To that end, seven different group of parameters are defined to analyze the effects of the system parameters. The results have shown that the required torque takes on both positive and negative values inside one cycle, consistent with the literature. However, the mechanism driven by an electrical motor cannot provide both positive and negative torque. One solution would be to utilize a flywheel to compensate for the energy fluctuations. Other studies available in the literature suggest using suitable springs for the same purpose [6].

Discussion above and further numerical experiments with the dynamic model indicate that parameters involved cannot be selected arbitrarily. For example, as is also visible from the model that the joint force F_{34}^x is a function of the square of the angular speed, increasing the angular speed to high values may cause the joint force F_{34}^x to change its sense in different phases of the mechanism motion, hence causing also the contact surface between the intermediate slider and yoke to change its position from the bottom of the slot to its top, a condition which may not be desired as a design criterion. Therefore, in order to assure the right selection of the parameter values in the model, a thorough understanding of the mechanism behavior is essential through further investigations of the dynamic system model.

If the Scotch-yoke mechanism is going to be used within the framework of a conceptual design, then its constraints have to be taken into account as well. For instance, the output force generated in this mechanism may have to satisfy the requirements of a compression force in the sinusoidal form with desirable amplitude or maximum-minimum, and frequency characteristics. Yet other conditions may be that both the driving torque on the crank and the joint force F_{34}^{x} acting on the yoke sustain their signs throughout the operation of the mechanism. Stabilization of energy and speed, optimization in terms of desired criteria, inverse dynamic studies, where the resulting motion is analyzed in the mechanism under given actuation possibly constant input torque conditions, are issues and subjects of future work demanding answers for an effective use of the Scotch-yoke mechanism within the framework of a conceptual design.

5. REFERENCES

1. Nguyen, H.N. & Shieh, W.B. (2018). On the design of the gravity balancer using scotch yoke derivative mechanism. In Doroftei, I., Oprisan, C., Pisla, D., Lovasz, E. (eds) *New Advances in Mechanism and Machine Science. Mechanisms and Machine Science*, *57*. Springer, Cham.
2. Al Shami, E., Mayberry, L., Zhang, R. & Wang, X. (2023). A preliminary study of a novel wave energy converter of a Scotch Yoke mechanism-based power take-off. *Sustainable Energy Technologies and Assessments, 60*, 103533.
3. Hossain, Z. & Illias, H. (2022). Ocean wave energy harvesting via scotch yoke-based rotational generation. *AIUB Journal of Science and Engineering (AJSE)*, *21*(3), 167-175.
4. Subramanian, S.M., Murugesan, V., Perumal, A.V., Kumar, N.K.V.S., Anandhan, Y.S. & Arumugam, V. (2022). Design and analysis of the performance of scotch and yoke based two way pumping system. In *AIP Conf. Proc.*, *2527*(1), 030005.
5. Rivankar, S.N., Kattimani, P.C., Walke, G. & Nigalye, A. (2019). Scotch yoke mechanism for specimen polishing & microstructure analysis. *International Journal of Research in Advent Technology*, *7*(5), 455-459.
6. Kwon, S.-R. (2013). An adjustable scotch yoke mechanism for output torque regulation. *MSc Thesis.* School of Mechanical and Aerospace Engineering, The Graduate School, Seoul National University, Seoul, Korea, 41.
7. Prastiyo, W. & Fiebig, W. (2025). Balancing of slider-crank and Scotch-yoke mechanisms by the use of mechanical resonance: Simulation and experiment. *Simulation Modelling Practice and Theory*, *142*, 103137.
8. Rayed, A.M., Esakki, B., Banik, S.C. & Nahin, A. (2024). Computational modeling and optimization of a flapping mechanism based on the scotch yoke principle. *SAE Technical Paper, 2024*(01),2264.
9. Liang, Y. & Liu, Q. (2025). Dynamics simulation and analysis of scotch yoke mechanisms with opposed dual-piston and inclined slot configurations using ADAMS. *Journal of Physics: Conference Series*, *3098*, 012005.
10. Tao, D., Zhang, C., Li, N., Zheng, L. & Cao, Z. (2025). Design and analysis of guide mechanism driven by limacon gear. *U.P.B. Sci. Bull., Series D*, *87*(2), 59-68.
11. Apati, S. & Hegedus, G. (2023). Investigation and simulation of a scotch yoke mechanism. *MultiScience - microCAD International Multidisciplinary Scientific Conference - Special Issue Part I.*, *13*(2), 144-152.
12. Al-Hamood, A., Jamali, H.U., Abdullah, O.I. & Senatore, A. (2019). Dynamics and lubrication analyses of scotch yoke mechanism. *International Journal on Interactive Design and Manufacturing*, *13*, 901-907.
13. Tai, Y., Hua, X., Cheng, L., Huang, Z., Wang, S. & Wang, Z. (2024). Dynamic characterization and design of scotch yoke inerter with adjustable inertance for seismic isolation. *Journal of Structural Engineering*, *150*(11), 04024153.
14. Beyaz, A. & Dağtekin, M. (2018). Kinematic analysis of tractor engine crank-rod mechanism. *Çukurova Üniversitesi Mühendislik-Mimarlık Fakültesi Dergisi*, *33*(3), 93-100.
15. Sarıgeçili, M. İ. & Akçalı, İ.D. (2018). Dynamic modeling of slider-crank mechanism for selecting input parameters for desired piston speeds: Lumped mass approach. *Çukurova Üniversitesi Mühendislik-Mimarlık Fakültesi Dergisi*, *33*(4), 67-82.
16. Sarıgeçili M.İ., Dağdelen M. & Akçalı İ.D. (2022). Conceptual design of an axial fatigue loading machine. *3rd International 5 Ocak Congress on Applied Sciences*, Adana, 216-221.